DEVELOPMENT OF A HIGH RESOLUTION CAMERA AND OBSERVATIONS OF SUPERCONDUCTING CAVITIES

Y. Iwashita, Kyoto University, Uji, Kyoto, JAPAN
H. Hayano, KEK, Ibaraki, JAPAN
Y. Tajima#, Toshiba Corporation , Yokohama, Kanagawa, JAPAN

Abstract

An inspection system of the interior surface of superconducting RF cavities is developed in order to study the relation between the achievable field gradient and the defects of the interior surface. The achieved resolution is about 7 μm/pixel. So far there are good correlations between locations identified by thermometry measurements and positions of defects found by this system. The heights or depths can be also estimated by measuring wall gradients for some well-conditioned defects. The detailed system and the data obtained from the system are described.

INTRODUCTION

Superconducting (Sc) accelerating cavities have been developed more than ten years [i,ii,iii,iv]. The achieved accelerating field gradient has been increasing with progresses in fabrication process, while the yield of good cavities has to be improved more for real applications such as XFEL or ILC. In ILC case, we need more than 1,5000 9-cell-cavities with more than 35MV/m gradient and more than 80% yield. The main obstacles against the high gradient are thought to be Thermal Breakdown (TB) and Field Emission (FE), supposedly caused by defects on the surface with the size of order of 100 μm and 1μm, respectively [v]. An optical inspection should be a first choice for finding such defects [vi,vii]. In order to find the former defects in 100 μm sizes on the inner surface, we developed a high resolution camera. The achieved resolution is about 7μm/pixel and objects with more than several tens microns in size can be observed. This system revealed undiscovered defects at just the inner sides of the locations predicted by passband-mode and thermometry measurements.

CAMERA SYSTEM

Camera Cylinder

The inner surfaces of the Sc cavities are highly reflective but not perfect mirrors because of the surface finish. It makes the lighting for optical inspection very difficult; uniform lighting tends to give flat image that has no information. We finally use ElectroLuminescence (EL) sheets for the lighting. In order to achieve a non-destructive observation and keep the inner surface as clean as possible, the camera system has a profile of 50mm diameter cylinder (see Fig.1). This cylinder can be inserted into even the Low Loss (LL) Cavities, which have smaller iris diameters, while nothing protrudes from the cylinder. This structure has an advantage to a system that moves a tiny camera in the cavity cell, where a mis-operation of the camera movement might scratch the surface. The camera is installed in the cylinder looking towards the head where a mirror reflects the interior surface of a cavity. The mirror can be tilted by a pulse motor (PM) to show a surface other than the equator region. The focus is adjusted by motorized positioning of the camera keeping the optical length (working distance) between the object and the camera lens (see Fig.2). The camera used in this system is 1.5M pixel three layered CMOS color camera (CSF5M7C3L18NR, Toshiba-Teli) with c-mount for a lens interface, whose pixel size is 5×5 μm. A low distortion lens (VS-LD75, V.S. Technology Corp.) with extension tubes installed between the lens and the camera gives maximum magnification factor of 0.7×. Thus the maximum resolution at the object surface corresponds to 7μm/pixel. The illumination was performed by the EL sheets put on the cylinder surface; they are separated because the camera needs a window to look through. The EL sheets are further divided and turned on/off independently to change the position of the light source. This feature is useful in estimating defect heights, which will be explained later. This structure cannot emit light from the

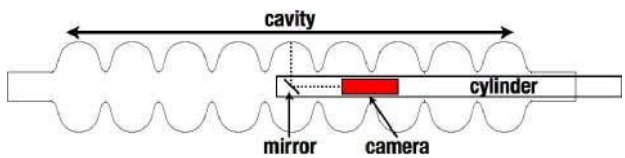

Figure 1 Schematic diagram of our cavity inspection system. A cavity swallows the camera cylinder by moving longitudinally. The cylinder does not move. The interior surface reflected in a mirror is observed. The mirror is located in front of the camera.

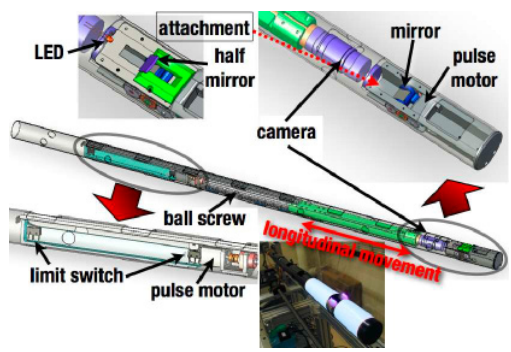

Figure 2 Inside of the camera cylinder. The inset shown in upper right corner shows the mirror and its drive PM. The camera moves for focal adjustment. The EL sheets for the illumination are shown at the bottom.

on leave from Kyoto University.

center (camera) and a surface normal to the line of the sight is difficult to be observed because the surface is almost a mirror. A half mirror with LED lamp installed on the line of the sight can illuminate such locations without interference of the sight.

Cavity Positioning Table

A cavity can be slid in longitudinal direction and rotated around its axis while the camera cylinder has fixed position so that the interior surface of every cell can be observed (see Fig.3). The longitudinal position of a cavity is known by the number of pulses fed to the PM, while the azimuthal coordinates is measured by the rotary encoder put on the edge of a cavity flange. Although the camera cylinder is fixed on the table, movement of the cavity during its positioning shakes the cylinder. This disturbs the observation during the swing because of the very narrow depth of field. A damper installed at the end of the cylinder helps to damp the swing quickly.

OBSERVATIONS

Zanon 84

The first cavity that was observed by the camera system was Z84 borrowed from DESY. While this cavity was diagnosed as Q-diseased at DESY, 27MV/m was recorded by passband-mode measurement and some cells out of 9 cells seem good. The 10mm-band regions on the equators were observed at 15μm/pixel resolution. Figure 4 shows a typical image obtained by the system. There were 35 spots whose radii were more than 100 μm in diameter. The population distribution shown in Fig.5 alludes to the existence of many more spots with smaller diameters. It should be mentioned that these spots are not just on the Electron Beam Welding (EBW) seam center but on the seam edge of the input coupler side.

AES001

AES001 from FNAL was the second cavity, whose surface was not barrel polished. It showed a quench at 15MV/m by TB while there was no FE[viii]. The quenched cells identified by the passband mode measurement were #3 and/or #7. A thermometry measurement further localized the hot spot positions at the equator regions in #3 cell (see Fig.6 left) and two hot spot locations at the thermosensors of #4 and #5 were

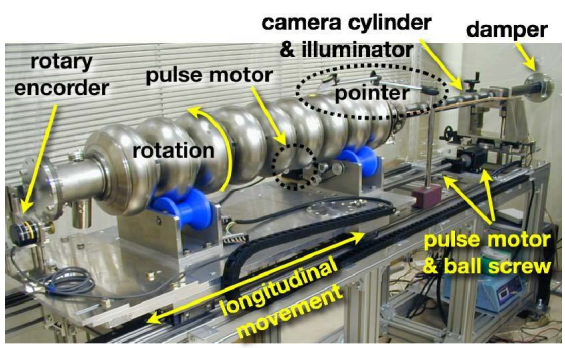

Figure 3 Overview of our inspection system.

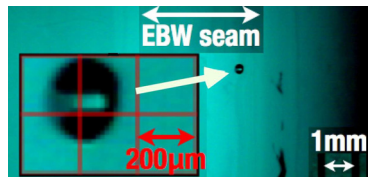

Figure 4 Typical image obtained for Z84. Many cat's eye shaped spots were observed.

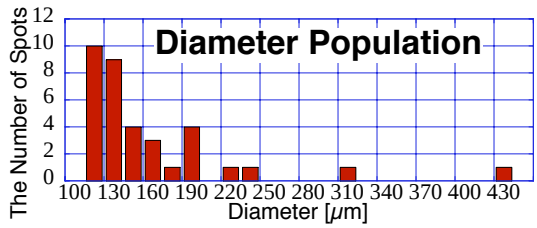

Figure 5 Population of diameter from Z84 observation.

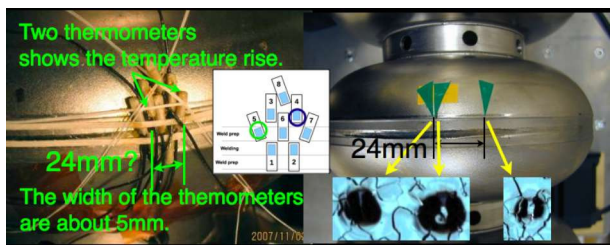

Figure 6 Positions of the two hot spots found at FNAL (left) and those found at Kyoto (right). The inset of left figure shows the location of the thermometers. The two thermometers (#4 and #5) that showed abnormal temperature rise are marked. (Courtesy of FNAL/JLAB.)

identified. We inserted the camera and observed the interior surfaces of these locations with about 7μm/pixel resolution and found cat's eye shaped defects at the locations just predicted by the thermometry (see Fig.6 right). The locations were identified as follows: 1) put a pointer just at the center of the camera view (off-cavity) 2) position the cavity to look at the defect and then 3) mark the location on the cavity pointed by the pointer (see Fig.7). The hot spot #5 had twin defects about 600μm in diameter and the hot spot #4 had a defect 400μm in diameter. Although these three spots have similar shape, cat's eye, the pupils (bars) in the twins were not clear

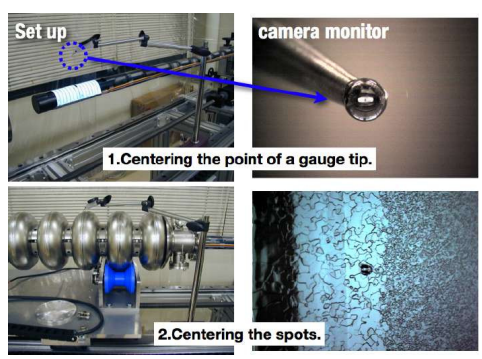

Figure 7 Pointer to confirm the position monitored by the camera on the exterior wall of a cavity.

maybe because of contaminations in them.

We also found defects at the equator region of the #7 cell, which was predicted by the passband mode measurement as TB source as shown in Fig.8. Twins are also found in the #3 cell. It should be noted that these defects are found at edges of EBW seams (including Z84 case). These locations are transition regions between completely melted region and the original region where the grain size changes. This may conclude a following speculation of the cause of the defects: when the Nb material was heated, impurities contained in the Nb made a bulge or its crater after eruption and they were left if they can not melt again in time to vanish, since the temperature at the transition region returns quickly. When the temperature and its duration is large enough, all such bulges would erupt and be assimilated. These were the only defects found in the AES001 but some smears, scratched, arc scars , etc. were observed.

HEIGHT MEASUREMENT

The camera images only show the cross section of the defects; there is no height information from the image itself. A tilt angle of a mirror can be estimated by knowing the location of the light source and the reflected angle. Integration of a tilt angle along a line gives the height profile of a defect. Fig. 9 shows the principle of the measurement [ix]. In order to realize the principle, the EL sheets are further divided as a stripe illuminator as shown in Fig.10, where each strip works independently. When the light band on the EL sheet runs along the axis, a bright point in a cat's eye pupil moves. Thus we can estimate the tilt angle of the mirror surface from the available angle information. Fig. 11 shows a typical result. The black curve in the left figure is the fitted differential Gaussian, from which the height of the spot is 40[μm]. The black curve in the right figure is the fitted Gaussian, from which the height of the spot is 42[μm].

CONCLUDING REMARKS

The good correlation between the thermometry and the locations of defects are promising for efforts towards better production yield of the cavity with high gradient. This system can be delivered worldwide to improve cavity fabrication processes and their yields. Further improvements are under trial, such as more resolutions and easy manipulations. We thank all collaborators who helped us to achieve this work.

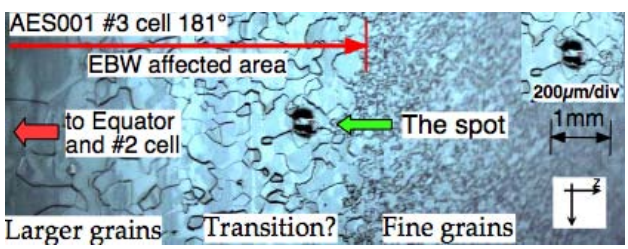

Figure 8 Cat's eye spot found at the equator region of #3 cell, 181deg. The diameter is about 400[μm].

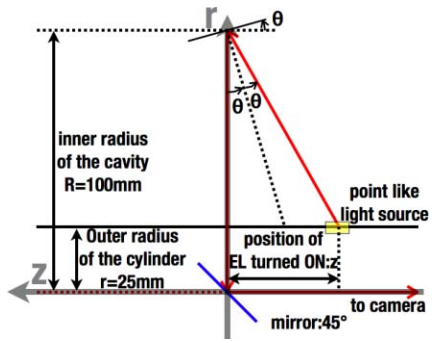

Figure 9 Schematic drawing of the wall gradient measurement. The wall gradient, the incident angle and the reflection angle are all the same. The value θ can be calculated from the position z of the illuminator.

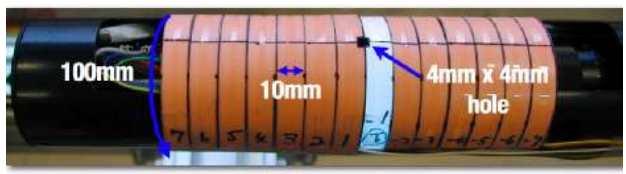

Figure 10 Stripe illuminator. The mirror is located under the hole between the two stripes numbered #1 and #-1. These fourteen stripes can be independently turned ON/OFF.

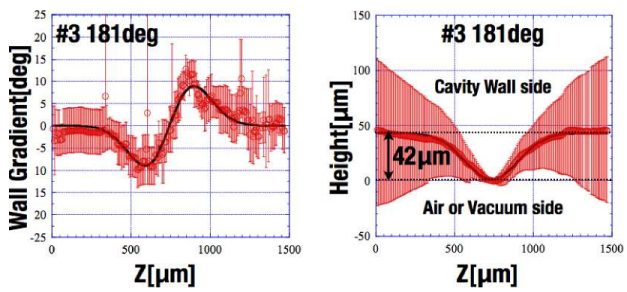

Figure 11 Gradient and height of the spot shown in Fig.8. The spot is a convex. The height is expressed by a relative value of the distance from the cavity axis.

REFERENCES

[i] H. Padamsee: IEEE Trans. Applied Superconductivity, **15**, 2005, p.2432.
[ii] H. Hayano: Proc. the 4th Annual Meeting of Particle Accelerator Society of Japan and the 32nd Linear Accelerator Meeting in Japan, 2007, p.218.
[iii] L. Lilje: Proc. LINAC 2002, Gyeongju, Korea, p.219.
[iv] J. Knobloch: IEEE Trans. Applied Superconductivity, **9**, 1999, p.1016.
[v] H. Padamsee, J. Knobloch and T. Hays: RF Superconductivity for Accelerators. New York: John Wily, 1998.
[vi] K. Saito: Proc. of the 21st Linear Accelerator Meeting in Japan, 1996, p.219.
[vii] T. Harden, M. Borden, A. Canabal, P. Pittman, T. Tajima: Proc. of PAC07, Albuquerque, New Mexico, USA, p.2409.
[viii] C. M. Ginzburg, R. L. Geng, J. Ozelis, D. A. Sergatskov, private communication.
[ix] Y. Tajima, Master's Thesis, Department of Physics, Kyoto University, 2007